Propene Oxidation and Hydrogenation on a Porous Platinum Electrode in Acidic Solution

Maria Bełtowska-Brzezinska,*,† Teresa Łuczak,† Helmut Baltruschat,‡ and Ulrich Müller‡

Department of Chemistry, A. Mickiewicz University, PL-60780 Poznań, Grunwaldzka 6, Poland and Institute of Physical and Theoretical Chemistry, University of Bonn, Römerstrasse 164, D-53117 Bonn, Germany

Received: July 24, 2002; In Final Form: February 20, 2003

The electrochemical reactivity of propene at the polycrystalline Pt/acidic solution interface was studied by on line differential electrochemical mass spectrometry (DEMS). It was shown that a relatively fast adsorption of hydrocarbon molecules on the electrode surface preceded their electroreduction and electrooxidation at $E <$ 0.2 V and $E >$ 0.6 V, respectively. The adsorbate consisted of associatively bonded propene, partially dehydrogenated C_3-hydrocarbon residues, as well as C_3-, C_2-, and/or C_1-oxygen-containing species in relative amounts dependent on the adsorption potential and the subsequent potential sequence. The maximum electrode coverage of 0.58 nmol cm^{-2} was achieved in the potential range 0.3−0.5 V, where the major part of the surface species was propene itself, oriented with the carbon chain almost parallel relative to the electrode/solution interface. The oxygenated C_3-species were formed favorably in the presence of coadsorbed water and/or OH species, at 0.5 V $< E <$ 0.8 V. Propane was identified as the main volatile product of the cathodic hydrogenation of the adsorbate. Additionally, the reductive decomposition of the oxygenated C_3-species yielded methane along with the C_2-oxygen-containing moieties remaining on the Pt surface and/or undergoing further fragmentation to the C_1-oxygen-containing residues. The only final volatile oxidation product of all the adsorbates was CO_2.

1. Introduction

A detailed knowledge of the electrochemical behavior of unsaturated hydrocarbons is of primary importance for development of appropriate sensors and for advanced electroorganic synthesis. Actually, most of the available information on this subject concerns the adsorption, cathodic hydrogenation, and anodic oxidation of ethene on Pt, showing a particularly high electrocatalytic activity among the transition metals.[1−15] In earlier papers, several possible mechanisms of the aforementioned processes were considered on the basis of the kinetic data obtained with the classical electrochemical methods, without any direct identification of reactive intermediates and reaction products.[1−6] Some preliminary information on the chemical properties of the ethene adsorbate formed on the Pt(111) electrode was elucidated ex situ, by means of Auger spectroscopy (AES) in a vacuum.[7,8] A comparison of the voltammetric charge density related to the electrocatalytic oxidation of terminal alkenes, preadsorbed on Pt(111) from the gas phase, with the molecular packing density obtained from AES signals revealed that the hydrocarbon species attached to the metal surface through the carbon−carbon double bond, stable at Pt in a vacuum, are also stable at a Pt/solution interface in the double layer potential range. Next, the Pt(100) ordered surface was found to exhibit a higher catalytic activity toward the ethene electroreduction than that of the Pt(111) surface.[9]

More recently, the nature of the ethene adsorbate on mono- and polycrystalline Pt electrodes was ascertained via on line differential electrochemical mass spectrometry (DEMS).[10−14] It was shown that the surface concentration of the species identified, that is π- and di-σ-bonded ethene, multibonded ethylidyne, and oxygen-containing residues, depends on the crystallographic and electronic metal structure as well as the electrode potential. A disordered structure of the ethene adlayer was revealed by scanning tunneling microscopy (STM).[15] In parallel, the reactivity of the adsorbates formed from ethene derivatives, benzene, cyclohexene, and ethyne was determined on poly- and monocrystalline Pt electrodes.[10−14,16]

To the best of our knowledge, though, for alkenes of C_3 or longer carbon chain, the on line or in situ spectroscopic investigation has so far been performed only for Au/solution[17,18] and Pt/gas interfaces.[8,19−22] But it is well-known, among others from the study of ethene, that the interaction of organics with Au is much weaker than that with Pt,[14] and furthermore there are marked differences in the structure of the species formed on the Pt surface upon adsorption from the liquid and gas phases.[7,14] This paper reports results of on line DEMS studies of the oxidation and reduction of propene on a porous Pt/PTFE electrode in acidic solution, undertaken to gain insight into the mechanism of these processes.

2. Experimental Section

DEMS measurements were carried out in a three-electrode cell with an inlet and outlet for solution, so that electrolyte exchange was possible without interrupting the potential control of the working electrode attached to the vacuum chamber of the computerized mass spectrometer Balzers QMG 511. Details of the DEMS technique together with calibration of the mass spectrometer for the compounds investigated (CO_2, C_3H_6, C_3H_8, and CH_4) were described previously.[11,12,14,16,23−25]

The working electrode of geometric area of 0.2 cm^2 was a porous Pt layer of 65 nm thickness, sputtered onto a PTFE membrane (Gore-Tex, pore size 0.02 μm, thickness 75 μm).

* Corresponding author. E-mail address: mbb@ amu.edu.pl. Fax: +48 61 8658008.
† A. Mickiewicz University.
‡ University of Bonn.

10.1021/jp021726f CCC: $25.00
Published on Web 05/15/2003

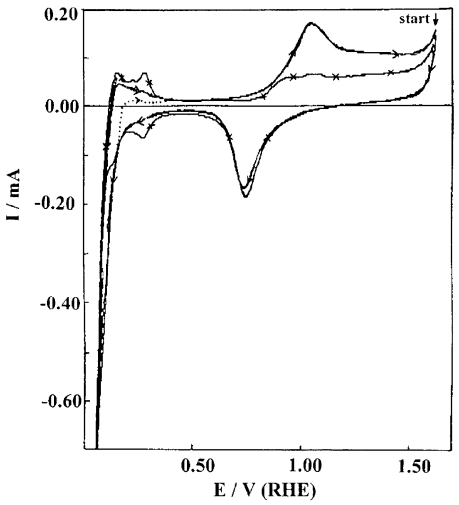

Figure 1. Cyclic voltammograms of a porous Pt electrode in 0.25 M H_2SO_4 + 2 × 10^{-2} M C_3H_6 upon stirring with gaseous propene. Cathodic potential limits, $E_{CPL} = -0.15$ V (solid line with arrows) and $E_{CPL} = 0.15$ V (dotted line overlapped on the solid line with arrows for $E > 0.4$ V); $dE/dt = 12.5$ mV s^{-1}. The CV of Pt in 0.25 M H_2SO_4 deaerated with argon is shown by the line with ×'s. Arrows indicate the start and direction of the potential sweep.

The counter electrode was a Pt wire. A reversible hydrogen electrode (RHE) served as the reference electrode. Prior to each experiment, the working electrode was activated in the supporting electrolyte solution (0.25 M H_2SO_4, deaerated with argon) by cycling in the potential range 0.07−1.5 V until a reproducible voltammogram was obtained. Next, the roughness factor (rf) of Pt was determined from the charge density corresponding to the adsorption−desorption of hydrogen, assuming that a hydrogen monolayer requires 0.210 mC/real cm^2.[26]

The mass spectrometric cyclic voltammograms (MSCVs), up to five *m*/*z* values, were recorded simultaneously with conventional cyclic voltammograms (CVs). Experiments were performed at room temperature in propene saturated electrolyte solution, constantly purged by gaseous reactant and after replacement of the reactant-containing electrolyte with pure supporting electrolyte (electrolyte exchange), following the adsorption at a constant potential E_{ad} (in the range 0.1−0.8 V) for the time t_{ad}. The latter procedure ensured that only the volatile products released during the oxidation or reduction of the preadsorbed species were detected in the positive and negative going sweep, respectively.

In the preceding paper[16] we described the procedures for determination of the electrode coverage (Θ), the number of electrons transferred per one carbon atom (n_{epm}) and per one Pt site (n_{eps}) upon the adsorbate oxidation, as well as the surface concentration (Γ/nmol per cm^2 of the real surface area) of volatile oxidation and reduction products.

Chemicals were used as received: propene, 99.99% (Linde); argon, 99.999% (Messer Griesheim); carbon monoxide, 99.99% (Messer Griesheim); sulfuric acid, suprapur (Merck). Solutions, made with Millipore MilliQ water, were deaerated with argon. All experiments were performed at room temperature.

3. Results

3.1. Electroreduction and Electrooxidation of Bulk Propene. Typical CVs of propene on a porous Pt electrode in an acidic medium saturated with the dissolved reactant (2 × 10^{-2} M) are presented in Figure 1. The electroreduction of propene at $E < 0.2$ V is manifested as a substantial increase in the cathodic current above that related to the electrosorption of hydrogen on the electrode investigated in pure electrolyte solution. As shown in Figure 2, the simultaneously obtained MSCVs for $m/z = 42$ ($[C_3H_6]^{\bullet+}$) evidence consumption of the reactant at the electrode/solution interface. Propane is the only volatile reduction product giving rise to the potential dependent ion currents for $m/z = 44$ ($[C_3H_8]^{\bullet+}$), 43 ($[C_3H_7]^+$), 41 ($[C_3H_5]^+$), 39 ($[C_3H_3]^+$), 29 ($[C_2H_5]^+$), 28 ($[C_2H_4]^+$), 27 ($[C_2H_3]^+$), and 15 ($[CH_3]^+$), with relative intensities characteristic of this saturated hydrocarbon. The representative MSCVs for $[C_3H_8]^{\bullet+}$ and $[C_2H_5]^+$ (at $E < 0.2$ V) are given in Figures 3 and 4, respectively. The maximum observed in these mass signals at $E \approx 0.1$ V corresponds to production of propane from propene preadsorbed on the Pt surface after the electroreduction of the platinum oxide is completed. The electrode coverage with the unsaturated hydrocarbon is clearly ascertained by strong suppression of the faradaic current related to the hydrogen adsorption−desorption. It is particularly well visible in CVs obtained with the cathodic potential limit fixed at the onset of propene hydrogenation (e.g. $E_{CPL} \approx 0.15$ V, as in Figure 1). But at $E < 0$ V, the rate of propene electroreduction becomes much higher than that of its adsorption and diffusion from the bulk solution. This is well evidenced in Figures 3 and 4 by the potential independent ion currents corresponding to the propane evolution.

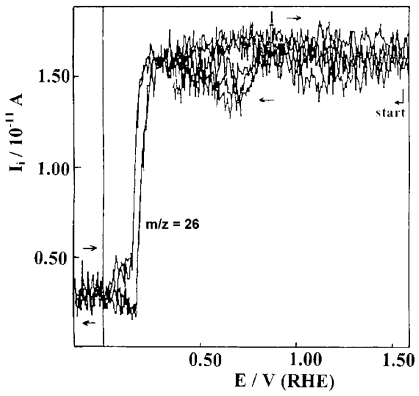

Figure 2. Mass spectrometric cyclic voltammograms for propene (*m*/*z* = 42) obtained in parallel with CVs in Figure 1 on a porous Pt electrode in 0.25 M H_2SO_4 + 2 × 10^{-2} M C_3H_6 stirred with gaseous reactant: $K^* = 0.95 \times 10^{-6}$; $dE/dt = 12.5$ mV s^{-1}. Arrows indicate the start and direction of the potential sweep.

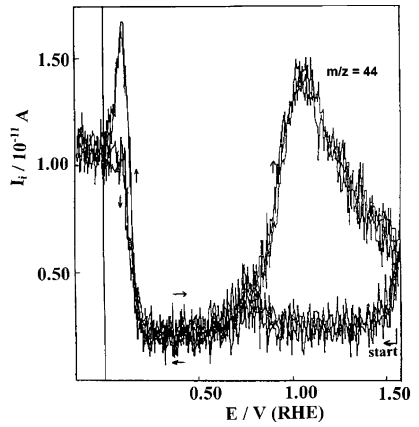

Figure 3. Mass spectrometric cyclic voltammograms for $m/z = 44$ obtained in parallel with CVs (see Figure 1) upon cathodic reduction of propene to propane (at $E < 0.2$V) and anodic oxidation of propene to CO_2 (at $E > 0.6$ V) on a porous Pt electrode in 0.25 M H_2SO_4 + 2 × 10^{-2} M C_3H_6 stirred with gaseous reactant: $K^* = 0.95 \times 10^{-6}$; $dE/dt = 12.5$ mV s^{-1}. Arrows indicate the start and direction of the potential sweep.

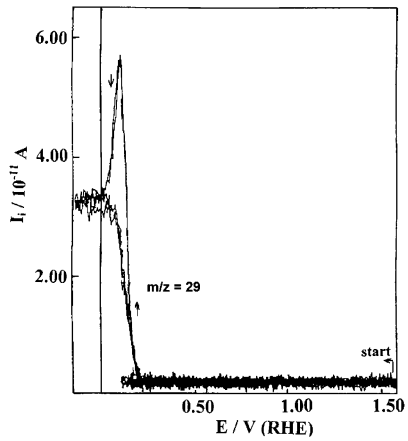

Figure 4. Mass spectrometric cyclic voltammograms for $m/z = 29$ (propane) obtained in parallel with CVs in Figure 1 and MSCVs in Figure 3 on a porous Pt electrode in 0.25 M H_2SO_4 + 2×10^{-2} M C_3H_6 stirred with gaseous reactant: $K^* = 0.95 \times 10^{-6}$; $dE/dt = 12.5$ mV s^{-1}. Arrows indicate the start and direction of the potential sweep.

As shown in Figure 1, the electrooxidation of bulk propene is reflected in the CVs as the broad anodic current peak within the potential range 0.6−1.6 V. Taking into regard the results of previous studies on the reactivity of other organic compounds on Pt,[10−14,16,27−30] it can be assumed that water molecules activated by the electric field at the Pt electrode/solution interface initially (0.6−0.9 V) act as oxygen donors in this reaction. A large majority of propene, however, is oxidized at $E > 0.9$ V when the Pt surface is substantially covered with the $(OH)_{ad}/(O)_{ad}$ species. The corresponding MSCVs for $m/z = 44$ ($[CO_2]^{\bullet+}$) displayed in Figure 3 and for $m/z = 28$ ($[CO]^{\bullet+}$) are the only ones which reveal the same features as the CVs at $E > 0.6$ V. Since no other potential dependent mass intensities were detected by checking MSCVs for various m/z values, it is obvious that CO_2 is the sole volatile product of propene oxidation, as was earlier reported for ethene[10−14] and ethyne.[16] No aldehyde or ketone was formed under the experimental conditions.

An interesting finding is that the anodic parts of both the CVs (Figure 1) and MSCVs for CO_2 (Figure 3) obtained at $E > 0.6$ V on a Pt electrode in the propene-saturated electrolyte solution closely resemble those related to the adsorbate oxidation, in the experiments with electrolyte exchange (see Figure 5 and the description in the next section). This shows that once the oxide layer is formed on Pt, only the propene species adsorbed earlier in the double layer region are oxidized. Propene readsorbs again after electroreduction of the oxide layer, which leads to some decrease of the educt signal ($m/z = 42$) at $E \approx 0.7$ V during the negative sweep (Figure 2).

3.2. Electrooxidation of Propene Adsorbate. Irreversibly bonded species remain on the Pt surface after adsorption of propene at a constant electrode potential (E_{ad}) followed by a replacement of the reactant-containing electrolyte with pure supporting electrolyte. The exemplary CVs in Figure 5A and the corresponding MSCVs in Figure 5B illustrate the effect of E_{ad} within the 0.1−0.8 V range on the faradaic charge density (Q_{ox}) and the ion charge density of $[CO_2]^{\bullet+}$ ($Q_{MSCV,m/z=44}$) released during the direct adsorbate oxidation (in the first positive sweep) after electrolyte exchange.

As follows from the data summarized in Tables 1 and 2 (entries 1 and 1′), the highest and almost constant electrode coverage with organic species is reached at E_{ad} between 0.3 and 0.5 V. The respective number of electrons transferred per surface carbon atom oxidized to CO_2, $n_{epm} \approx 5.9$, corresponds

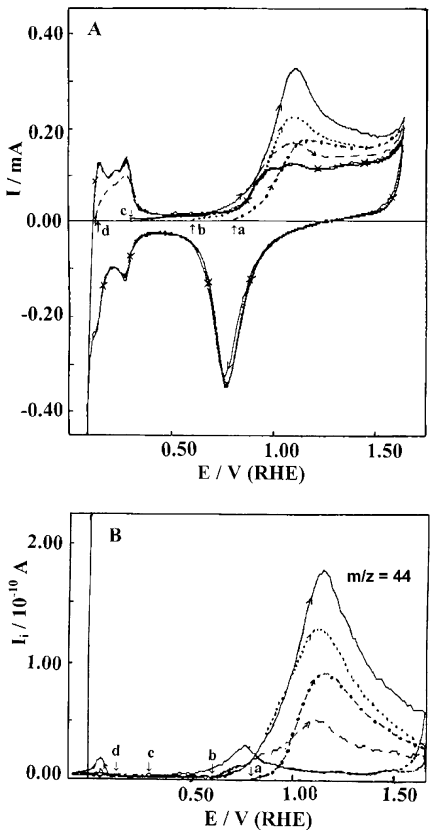

Figure 5. Direct oxidation of propene preadsorbed on a porous Pt electrode in 0.25 M H_2SO_4 + 2×10^{-2} M C_3H_6 at various E_{ad} = const (t_{ad} = 300 s) and succeeding reduction of the anodically undesorbable residues: (A) CVs and (B) MSCVs for CO_2 at $E > 0.6$ V and C_3H_8 at $E < 0.2$ V, obtained upon the first positive sweep and the following negative sweep after electrolyte exchange at (a) $E_{ad} = 0.8$ V (dotted-dashed line), (b) $E_{ad} = 0.6$ V (dotted line), (c) $E_{ad} = 0.3$ V (solid line), and (d) $E_{ad} = 0.14$ V (dashed line). $dE/dt = 25$ mV s^{-1}; $K^* = 0.7 \times 10^{-5}$. CVs of Pt in 0.25 M H_2SO_4 are given by the line with ×'s. Arrows indicate the start and direction of the potential sweep.

TABLE 1: Faradaic Charge Density (Q_{ox}), Ion Charge Density Corresponding to the CO_2 Mass Signal ($Q_{MSCV,m/z=44}$), the Surface Concentration of CO_2 Related to the Real Pt Area (Γ_{CO_2}), and the Number of Electrons (n_{epm}) Transferred for One Surface Carbon Atom during Oxidation of Propene Species Preadsorbed on a Porous Pt/PTFE Electrode in 0.25 M H_2SO_4 + 2×10^{-2} M C_3H_6 at Various E_{ad} (t_{ad} = 180 s), after Electrolyte Exchange: $K^* = 7 \times 10^{-6}$

E_{ad}/ V	$Q_{MSCV,m/z=44}$/ (nC cm^{-2})	Q_{ox}/ (mC cm^{-2})	Γ_{CO_2}/ (nmol cm^{-2})	n_{epm}
0.12	1.2	1.01	0.48	5.9
0.20	1.8	1.52	0.73	5.9
0.30	2.7	2.27	1.09	5.9
0.40	2.7	2.27	1.09	5.9
0.50	2.7	2.15	1.09	5.6
0.60	2.2	1.52	0.89	4.8
0.70	1.6	0.89	0.65	3.9
0.75	1.4	0.65	0.56	3.2

well to that expected for the complete oxidation of propene according to $C_3H_6 + 6H_2O = 3CO_2 + 18H^+ + 18e$. By taking into account the similar $n_{eps} \approx 5.8$ value, it is plausible to conclude that the adlayer formed in the potential range considered consists predominantly of the associatively bonded reactant molecules, blocking three adjacent Pt sites with the C_3-carbon chain arranged almost parallel to the metal surface. Indeed, the total amount of CO_2 evolved upon a complete adsorbate oxidation in the first two voltammetric cycles, between

TABLE 2: Ion Charge Density Corresponding to Mass Signals (Q_{MSCV}) and the Surface Concentration Related to the Real Pt Area (Γ) of Volatile Products of Electrooxidation and Electroreduction of Propene Species Preadsorbed on a Porous Pt/PTFE Electrode in 0.25 M H_2SO_4 + 2 × 10^{-2} M C_3H_6 at Various E_{ad}, after Electrolyte Exchange

	adsorption and sweep conditions	*m/z*	product	Q_{MSCV}/(nC cm^{-2})	Γ/(nmol cm^{-2})
1.	(a) positive sweep starting from E_{ad} = 0.3 V after t_{ad} = 660 s	44	CO_2	3.52	1.42
	second positive sweep after negative sweep (the cathodic potential limit at 0.15 V)	44	CO_2	0.8	0.32
	(b) positive sweep starting from E_{ad} = 0.3 V after t_{ad} = 300 s	44	CO_2	3.11	1.25
2.	negative sweep starting from	44	propane	0.35	0.37
	E_{ad} = 0.3 V after t_{ad} = 300 s	29	propane	1.29	
3.	positive sweep after negative sweep starting from E_{ad} = 0.3 V after t_{ad} = 300 s				
	total amount	44	CO_2	0.71	0.28
	partial amount for 0.6 V < E < 0.9 V	44	CO_2	0.21	0.085
4.	negative sweep after positive sweep starting	44	propane	0.048	0.05
	starting from	29	propane	0.18	
	E_{ad} = 0.3 V after t_{ad} = 300 s	15	methane	0.018	0.008
1′	positive sweep starting from E_{ad} = 0.6 V after t_{ad} = 300 s	44	CO_2	2.33	0.93
2′	negative sweep starting from	44	propane	0.21	0.23
	E_{ad} = 0.6 V after t_{ad} = 300 s	29	propane	0.79	
		15	methane	0.113	0.057
3′	positive sweep after negative sweep starting from E_{ad} = 0.6 V after t_{ad} = 300 s				
	total amount	44	CO_2	1.15	0.46
	partial amount for 0. 6 V < E < 0. 9	44	CO_2	0.57	0.23

0.2 and 1.6 V (Table 2, entry 1a), indicates that the surface concentration of propene species on the porous Pt electrode after t_{ad} = 660 s at E_{ad} = 0.3 V achieves the maximum value of Γ_{max} = 0.58 nmol per cm^2 of the real electrode area. This molecular packing density is comparable to that obtained theoretically and experimentally for the monolayer of propene lying flat on Pt-(111) after adsorption from the gas phase.[8] For t_{ad} = 180 s and t_{ad} = 300 s the coverage degree ($\Theta = \Gamma/\Gamma_{max}$) of the investigated Pt electrode at E_{ad} = 0.3 V is found to be ~0.77 (Table 1) and ~0.88 (Table 2, entry 1b), respectively.

If the cathodic potential limit after the first oxidation cycle starting from E_{ad} = 0.3−0.5 V is positive enough to prevent any reductive desorption, about 10−20% of the preadsorbed surface species get oxidized in the second voltammetric cycle, at E > 0.9 V. This residual adsorbate, characterized by $n_{epm} \approx$ 5, can still be reduced to propane at the electrode potentials below 0.2 V (see Figure 5B). Therefore, it is obvious that the carbon skeleton of propene remains intact upon adsorption, although certain C−H bonds are cleaved, leaving the C_3H_x residues more strongly bonded on Pt than propene itself.

Partial adsorbate oxidation or its reductive desorption, occurring competitive to the reactant adsorption, leads to lower coverages with organic species and thus Q_{ox} as well as $Q_{MSCV,m/z=44}$ for E_{ad} > 0.5 V or for E_{ad} < 0.3 V (see Figure 5 and Table 1), respectively. However, the almost constant value of $n_{epm} \approx$ 5.9 for all E_{ad} below 0.5 V still indicates molecular propene as the dominant surface species over the whole potential region of hydrogen adsorption−desorption. On the other hand, a stronger decrease in Q_{ox} than that in $Q_{MSCV,m/z=44}$, along with a change of E_{ad} above 0.5 V and a gradual diminishing of the n_{epm} value, shows that increasing amounts of chemisorbed species must be in a higher oxidation state than the reactant molecules. This is additionally corroborated by the observation of anodic current transients upon introducing propene solution into the cell at E_{ad} between 0.5 and 0.8 V, while only current spikes toward the positive direction were found at lower adsorption potentials. In particular, for n_{epm} < 5 one should expect that the adsorbate involves the C_3-oxygen-containing species besides the partially dehydrogenated propene residues and molecular hydrocarbon. As CO_2 was detected in trace amounts only, any substantial breaking of the C_3-carbon chain during the propene adsorption up to E_{ad} of about 0.8 V can be ruled out.

3.3. Electroreduction of Propene Adsorbate. A large majority of the chemisorbed species, indicated above as associatively bonded propene, undergoes electroreduction during the first negative sweep after the electrolyte exchange (see CVs in Figure 6A) and desorbs as propane followed by the MSCVs (at E < 0.2 V) for $[C_3H_8]^{\bullet+}$ (Figure 6B), $[C_2H_5]^+$ (Figure 7A), $[CH_3]^+$ (Figure 7B), as well as $[C_3H_7]^+$, $[C_3H_5]^+$, $[C_3H_3]^+$, $[C_2H_4]^+$, and $[C_2H_3]^+$. Methane is the only additional volatile reduction product formed in the experiments with 0.5 V < E_{ad} < 0.8 V, high enough to enable the oxygen incorporation into the propene adsorbate via a reaction with coadsorbed water and/or OH species. As shown in Figure 7B, the mass signal for $[CH_3]^+$ after propene adsorption at E_{ad} = 0.6 V consists of the overlapping fragmentation components of methane and propane, while for E_{ad} = 0.3 V it reflects the evolution of pure propane only. Since, for all E_{ad} considered, all other above-mentioned potential dependent mass signals correspond to the fragmentation probability of propane (see Figures 6B and 7A), we can in particular exclude the formation of ethane and/or long-chain saturated hydrocarbons.

In Table 2 (entries 2 and 2′) one can find the amount of evolved propane for two selected E_{ad} values (0.3 and 0.6 V) as well as that of methane for E_{ad} = 0.6 V. As expected, the production of propane decreases in parallel with the appearance of methane among the reduction products. Accordingly, the MSCVs in Figures 6B and 7A display a markedly lower ion current for $[C_3H_8]^{\bullet+}$ (m/z = 44) and for $[C_2H_5]^+$ (m/z = 29) during the negative sweep after the reactant adsorption at E_{ad} = 0.6 V, in comparison with that for E_{ad} = 0.3 V. This provides additional evidence for a decrease in the surface concentration of molecularly adsorbed propene along with an increase in the electrode coverage with the oxygenated C_3-species.

Although the Pt surface becomes increasingly free from the organic adsorbate at potentials negative to 0.2 V, the cathodic desorption is not complete even if the electrode potential was

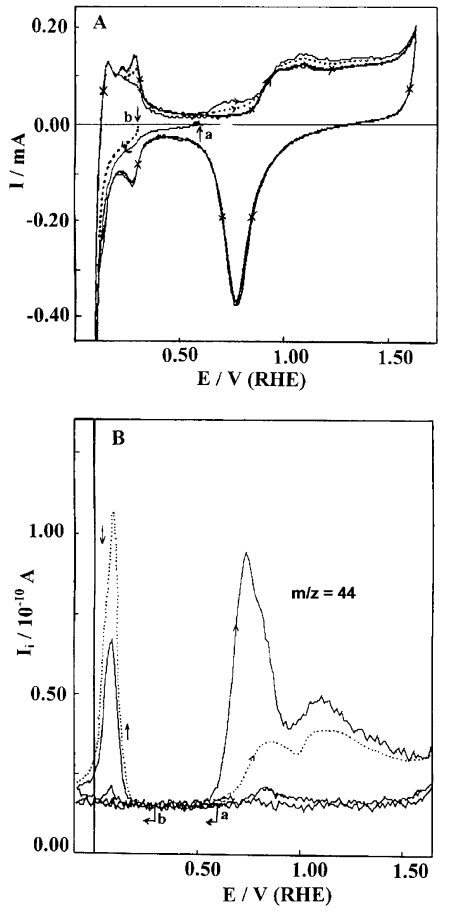

Figure 6. Direct reduction of propene preadsorbed on a porous Pt electrode in 0.25 M H_2SO_4 + 2 × 10^{-2} M C_3H_6 at various E_{ad} = const (t_{ad} = 300 s) and succeeding oxidation of the cathodically undesorbable residues: (A) CVs and (B) MSCVs for C_3H_8 at E < 0.2 V and CO_2 at E > 0.6V, obtained upon the first negative sweep and the following positive sweep after electrolyte exchange at (a) E_{ad} = 0.6 V (solid line) and (b) E_{ad} = 0.3 V (dotted line). E_{CPL} = −0.09 V; dE/dt = 25 mV s^{-1}; K^* = 0.7 10^{-5}. CVs of Pt in 0.25 M H_2SO_4 are given by the line with ×'s. Arrows indicate the start and direction of the potential sweep.

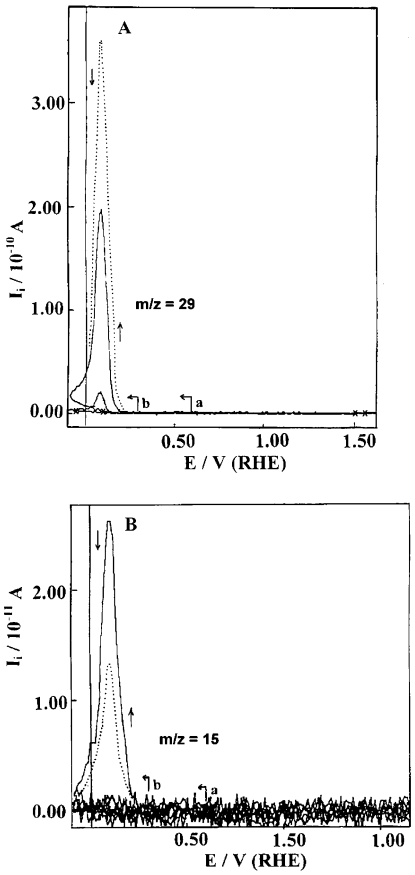

Figure 7. Direct reduction of propene preadsorbed on a porous Pt electrode in 0.25 M H_2SO_4 + 2 × 10^{-2} M C_3H_6 at various E_{ad} = const (t_{ad} = 300 s): (A) MSCVs for C_3H_8 (m/z = 29) and (B) MSCVs for CH_4 (m/z = 15), obtained in parallel with CVs in Figure 6A and MSCVs in Figure 6B upon the first negative sweep after electrolyte exchange at (a) E_{ad} = 0.6 V (solid line) and (b) E_{ad} = 0.3 V (dotted line). dE/dt = 25 mV s^{-1}. Arrows indicate the start and direction of the potential sweep.

held for a long time in the region of hydrogen evolution (i.e. at E = −0.1 V). Consequently, the overall amount of the volatile products formed upon the direct adsorbate electroreduction is to some extent lower than that expected on the basis of the amount of CO_2 evolved during the direct electrooxidation (Table 2, entries 1, 1′ and 2, 2′). As follows from the CVs in Figure 6A and the MSCVs in Figure 6B, part of the cathodically undesorbable residues can be removed from the Pt electrode during the succeeding positive sweep in the potential range 0.6−0.9 V, characteristic of the oxidative desorption of CO and/or alcohol-like species.[7,11−14,16,24] The remaining residual adsorbate gets oxidized at higher electrode potentials (E > 0.9 V), typical of the hydrocarbon fragments. The number of electrons released per each adsorbed carbon atom converted to CO_2 is equal to $n_{epm} \approx 3.7$ and $n_{epm} \approx 5$ in the former and latter potential ranges.

Interestingly, an appreciable rise in the electrode coverage with the residual oxygenated species showing the CO/alcohol-like electrochemical behavior accompanies the methane evolution, along with propane, upon the direct electroreduction of the adsorbate including the oxygenated C_3-species formed at E_{ad} > 0.5 V. It is manifested as an enhanced production of CO_2 around 0.7 V after inversion of the sweep direction. The respective charge density Q_{ox} and in particular the ion charge density $Q_{MSCV,m/z=44}$ for $[CO_2]^{\bullet+}$ are in this case distinctly larger than those obtained for E_{ad} < 0.5 (Figure 6; Table 2, entries 3 and 3′), in the absence of the oxygenated propene species on the Pt surface. Furthermore, a comparison of the MSCVs in Figure 5B with those in Figure 6B reveals that an amount of CO_2 around 0.7 V is negligibly small when the adsorbate is oxidized without a preceding cathodic reduction. Therefore, we conclude that the great majority of the CO/alcohol-like residues must be formed simultaneously with CH_4, via the reductive decomposition of the preadsorbed C_3-oxygen-containing species. This interpretation is supported by the fact that the surface concentration of CO_2 generated from the cathodically undesorbable oxygen-containing residues after the propene adsorption at E_{ad} = 0.6 V is about 2.5 times larger than that of CH_4 evolved in the hydrogen region {[Γ_{CO_2} for 0.6 V < E < 0.9 V (entry 3′ in Table 2)] − [Γ_{CO_2} for 0.6 V < E < 0.9 V (entry 3)]}/[Γ_{CH_4} (entry 2′)] ≈ 2.5. Thus, the same should be the ratio of the number of carbon atoms remaining strongly bonded on the electrode surface and that hydrogenated to methane after abstraction from the oxygenated C_3-species.

Note that a trace amount of methane was observed also during the negative sweep following the direct positive sweep after the propene adsorption at E_{ad} < 0.5 V (Table 2, entry 4), although it was absent in the experiments with the direct electroreduction of the same adsorbate (Table 2, entry 2). This points to a formation of the adsorbed C_3-oxygen-containing species not only during adsorption at E_{ad} > 0.5 V but also upon anodic cycling in the PtOH region.

4. Discussion

The results summarized in the preceding sections provide an insight into the pathway of propene reduction and oxidation on a porous Pt electrode. The evidence is given that a relatively fast irreversible reactant adsorption is involved in the initial step of these processes. Quantitative analysis of the CVs and MSCVs for a variety of *m*/*z* mass signals shows that the amount and nature of the surface species and, consequently, the composition of the final reaction products depend strongly on the adsorption potential and the subsequent potential sequence.

The dominant adsorbate over a relatively large E_{ad} range (0−0.8 V) is proved to be the associatively bonded propene, which quantitatively desorbs as propane in the hydrogen adsorption−desorption region. A plausible reason for the irreversible adsorption of the horizontally oriented propene molecules, as suggested by the maximum coverage value (58 nmol cm^{-2}), is the involvement of their π and σ orbitals in the donor−acceptor interaction with Pt having half-filled d orbitals. Earlier, the π− and di-σ-bonded species were identified by LEED, HREELS, TDS, XPS, and NEXAFS for ethene, ethyne, and propene adsorbed from the gas phase on Pt(111), Pt(210), and Pt supported on Al_2O_3.[19,31−37] Additionally, DEMS measurements have demonstrated that the π-bonded ethene can be displaced from the metal surface by Cu UPD, I^-, or CO while the di-σ-bonded ethene remains adsorbed on the polycrystalline Pt electrode.[38,39]

It is almost certain that the sp^2 toward sp^3 rehybridization of the C atom's orbitals at the double bond, accompanying the coordination of propene molecules to Pt surface sites, is additionally enhanced by the electric field at the electrode/solution interface due to the potential-induced donation and/or "back-donation" of the electron density between the metal and the organic compound. This is a reason for the relatively easy hydrogenation of propene to propane at $E < 0.2$ V as well as abstraction of hydrogen at E between 0.2 and 0.5 V followed by incorporation of oxygen into the adsorbate at 0.5 V $< E <$ 0.8 V and/or splitting of the carbon backbone upon conversion to CO_2 at more positive electrode potentials.

Earlier, a considerable weakening of the double C to C bond strength along with increasing positive electrode potential has been elicited using SERS/FTIRS techniques and EHMO calculation for alkenes adsorbed on Au and/or Ag.[18,40−46] However, the latter (group IB) metals are characterized by substantially poorer adsorptive properties than those of the transition metals and thus can be employed as catalysts of a partial electrooxidation of bulk hydrocarbon only. In contrast to the case for Pt, the main oxidation products of propene on a porous Au electrode were reported to be 2-propanone and ethanal, while a fission of the hydrocarbon backbone and CO_2 evolution occurred to a minor extent.[18] Ethanal and acetic acid were formed from ethene oxidized at the same electrode.[44,45]

On Pt, partial oxidation of propene also occurs. But, as for ethene,[10−14] the resulting species stay strongly bonded at the metal surface, giving rise to a higher average oxidation state ($n_{epm} \leq 5$) of the adsorbate (see Table 1) than that characteristic of the reactant molecules ($n_{epm} = 6$). This is in accordance with the volcano type behavior of metal catalysts, which means that high adsorption energy, on one hand, favors a reduction of the activation energy for dehydrogenation of organic molecules but, on the other hand, leads to a decrease in the overall catalytic activity due to unfavorable desorption of the reaction products. However, the possibility to desorb a major part of the surface species as propane allows us to gain information on the nature of the remaining adsorbate.

As shown in section 3.2, a certain amount of partially dehydrogenated propene residues appears on a Pt electrode already in the potential range of hydrogen adsorption−desorption, at $E_{ad} < 0.5$ V. Since the carbon skeleton remains intact, the $n_{epm} \approx 5$ value characteristic of this adsorbate implies the formation of the C_3H_x residues with the average number of H atoms equal to $\bar{x} = 3$. In fact, the adlayer may comprise a variety of species at a different degree of dehydrogenation and/or intramolecular rearrangement, from C_3H_5

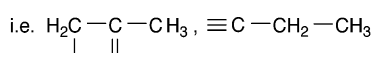

through C_3H_4

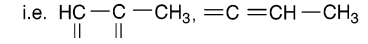

to C_3H_3

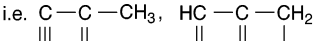

and other more dehydrogenated propene fragments, identified on Pt after adsorption from the gas phase.[19−22] This residual adsorbate, most probably due to the multiple bonding to Pt, is relatively strongly adsorbed and thus gets oxidized to CO_2 in the second voltammetric cycle (at $E > 0.9$ V) and/or reductively desorbed as propane (at $E < 0.2$ V) in the O- and/or H-rich environment, respectively.

Although the general propene behavior is similar to that reported for ethene,[10−14] there are some essential differences in the reactivity of the adsorbed species originating from these two compounds. Possibly due to sterical hindrance of the CH_3 group, the dimerization reaction does not occur among the partially dehydrogenated propene adsorbates. For ethene, this reaction was manifested by the presence of butane along with ethane among the hydrogenation products.[11,13,14] Furthermore, a comparison of CVs shown in Figure 5A with those obtained for ethene[38] revealed that the oxidation of the adsorbed propene takes place at somewhat higher positive electrode potentials. The same was found also in the steady-state current−potential relationships obtained for propene and ethene on platinized Pt.[1] A plausible reason might be a stronger competition of the former compound with H_2O/OH_{ad} species indispensable for CO_2 production and/or a higher activation energy of the oxidative desorption of propene species than that of ethene. This would be in line with a general trend of an increase in the adsorption affinity with a growing length of the carbon chain, which was found for various organic/metal systems.[8,47,48] Additionally, the inductive effect of the electron-repelling CH_3 group in the propene molecule may favor charge donation from the π orbitals of the double C=C bond to the vacant orbitals of Pt.

According to the experimental data (see section 3.3), the partly oxidized propene adsorbate, formed at $E_{ad} > 0.5$ V, includes not only the above-mentioned hydrocarbon fragments but also the oxygenated C_3-surface species, which then decompose to C_1-/C_2-moieties in the potential region of hydrogen adsorption (see section 3.3). A convincing evidence of a reductive rupture of the C_3-carbon backbone is the appearance of methane among the reduction products at $E < 0.2$ V, along with a substantial amount of irreversibly adsorbed CO/alcohol-like moieties. As the amount of CH_4 is about 2.5 times lower than that of CO_2 (Table 2, entries 2′ and 3′), it is believed that the interaction of the preadsorbed C_3-oxygen-containing species with coadsorbed hydrogen results in abstraction and hydrogenation of C_1-hydrocarbon moieties, while the other two carbon

atoms are left on the Pt surface in the C_2-oxygen-containing residues strongly bonded to the Pt surface and/or in C_1-oxygen-containing species after further decomposition.

The evolution of methane and propane at the ratio of 1:4 after propene adsorption at $E_{ad} = 0.6$ V (Table 2, entry 2′) indicates that about 20% of the C_3-adsorbate contains oxygen in its structure. Since ethane does not appear among the volatile reduction products, it is obvious that the reaction pathway leading to the oxygenated C_3-surface species (at $E > 0.5$ V) begins with formation of 2-propanol related species through the oxidative cleavage of the C−H bond at the 2C position in propene along with addition of the hydroxyl group on the same C atom:

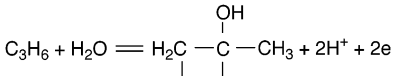

The progressive oxidation of the latter species may then lead to more dehydrogenated alcohol-like structures

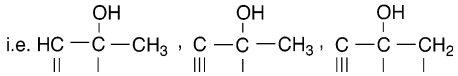

The subsequent formation of the 1,2-diol related species

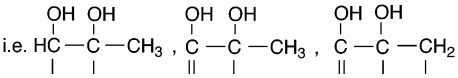

as well as oxidation of some alcohol functional groups to carbonyl groups and/or their dissociation to alcoxyl groups is also possible.

An alternative pathway that involves addition of a hydroxyl group on the 1C position of propene can be ruled out. Such a reaction would cause formation of 1-propanol-like species, which easily split into CO and C_2-hydrocarbon residues, yielding ethane during cycling in the hydrogen region.[14,49−51] In contrast, the parent C_3-structure is known to be retained in the adsorbate formed on Pt from 2-propanol.[49,51,52]

As already mentioned, the reductive decomposition of the oxygenated C_3-species in the hydrogen region yields methane and the C_2-oxygen-containing residual adsorbate responsible for production of CO_2 in the potential range 0.6−0.9 V with $n_{epm} = 3.7$. This n_{epm} value implies the formation of C_2H_xO and/or $C_2H_xO_2$ residues with the average number of hydrogen atoms equal to $\bar{x} = 1-2$ and/or $\bar{x} = 3-4$, respectively. In fact, the cathodically nondesorbable adsorbate may be composed of several species at a various degrees of dehydrogenation, with x between 5 and 0. In similar experiments with ethene,[10−14] the n_{epm} was ≈2 and, therefore, the formation of adsorbed CO was assumed. Interestingly, the $n_{epm} = 3.7$ for the C_2-oxygen-containing species derived from propene is close to that observed upon the direct oxidation of adsorbed ethanol around 0.7 V ($n_{epm} \approx 4$).[12] The species such as

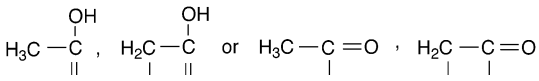

thus are probable. But in ref 12, it was shown with the use of ethanol (1-^{13}C) that also the 2-C atoms contribute to the formation of CO_2 in the potential range considered. Analogously, in the case of propene, not only the 2-C atom but (in part) also the 3-C atom will be oxidized, probably via the adsorbed CO as intermediate. This suggestion is supported by the amount of

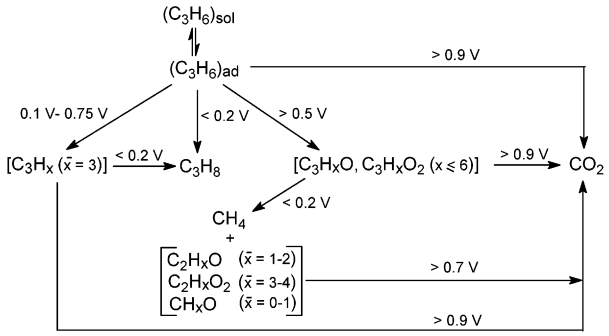

Figure 8. Propene surface reactions on a porous Pt electrode in acidic medium.

CO_2 formed around 0.7 V, which is ∼2.5 larger than that of the evolved CH_4.

Similarly to the hydrogenative cleavage of the first C to C bond within the initially formed oxygenated C_3-adsorbate, it should be possible to split methane from the resulting C_2-oxygen-containing structures mentioned above. Such a reaction occurred within the ethanol adsorbate.[12] Therefore, one might expect the CO_2 to CH_4 ratio to be the inverse of that found experimentally. The reason for these discrepancies may be 2-fold: either the hydrogenative splitting of the C−C bond does only occur when both C atoms are bound to the Pt surface and/or the H_3C group is also slowly oxidized to an alcohol group. Hydrogenative splitting of diol species should then lead to adsorbed CHO, COH, and/or CO species.[51,53]

Figure 8 summarizes the likely adsorbate states and electrocatalytic reactions of propene. The first step in both the electroreduction and electrooxidation processes involves an irreversible adsorption of the hydrocarbon molecules on Pt, connected with some transformation of the C to C double bond toward a single bond. The reductive addition of hydrogen to the associatively bonded propene and/or to the corresponding partially dehydrogenated hydrocarbon residues (C_3H_x) results in production of propane. A progressively stronger interaction between the organic species and Pt, along with the shift of the electrode potential in the positive direction, favors a simultaneous cleavage of certain C−H bonds of propene and formation of 2-propanol (C_3H_xO) and/or 1,2-propanediol ($C_3H_xO_2$) related species via the reaction with surface water. Further oxidation of these adsorbates to ketone-like species is also possible. Next, the reductive decomposition of the oxygenated C_3-species in the presence of coadsorbed hydrogen produces methane and cathodically nondesorbable C_2H_xO, $C_2H_xO_2$, and/or CH_xO residues. All the surface species, the molecularly adsorbed propene, hydrocarbon fragments, and oxygen-containing residues, get completely converted to CO_2 in the presence of the superficial PtOH layer. Further mechanistic information can be expected from DEMS studies of isotopic labeled compounds.

5. Conclusions

Propene can be effectively adsorbed in the potential range between 0.3 and 0.5 V and thereafter quantitatively reduced to propane in the hydrogen adsorption/evolution region (at $E <$ 0.2 V) or oxidized to CO_2 and H_2O in the $Pt(OH)_{ad}/Pt(O)_{ad}$ region (at $E > 0.9$ V).

Evidence is provided that the amount and nature of the adsorbate and, consequently, the composition of the final reaction products vary strongly with the electrode potential. However, the C_3-carbon skeleton remains preserved in a large majority of the surface species formed below 0.8 V. Between

0.3 and 0.5 V, the Pt electrode is covered to a maximum extent corresponding to a monolayer of propene species oriented with the carbon chain almost parallel to the metal/solution interface. Some chemisorbed 2-propanol and/or 1,2-propanediol related species are formed preferentially at *E* above 0.5 V, via the oxidative cleavage of certain C−H bonds of propene along with addition of hydroxyl groups from coadsorbed water. The C_3-oxygen-containing species undergo reductive decomposition in the hydrogen adsorption−desorption region, giving methane and cathodically nondesorbable C_2- and/or C_1-oxygen-containing moieties, which get oxidized in the potential range characteristic of the adsorbed CO.

Acknowledgment. This work was performed within a research project supported by the Committee for Scientific Research (KBN), Poland, Deutsche Forschungsgemeinschaft (DFG), and Deutscher Akademischer Austauschdienst (DAAD), Germany.

References and Notes

(1) Bockris, J. O'M.; Wroblowa, H.; Gileadi, E.; Piersma, B. J. *Trans. Faraday Soc.* **1965**, *61*, 2531−2545.
(2) Gilman, S. *Trans. Faraday Soc.* **1966**, *62*, 466−480.
(3) Gilman, S. *Trans. Faraday Soc.* **1966**, *62*, 481−493.
(4) Fujikawa, K.; Kita, H.; Miyahara, K. *J. Chem. Soc., Faraday Trans. 1* **1973**, *69*, 481−499.
(5) Fujikawa, K.; Katayama, A.; Kita, H. *J. Chem. Soc., Faraday Trans. 1* **1974**, *70*, 1−13.
(6) Fujikawa, K.; Kita, H.; Miyahara, K.; Sato, S. *J. Chem. Soc., Faraday Trans. 1* **1975**, *71*, 1573−1581.
(7) Wieckowski, A.; Rosasco, S. D.; Salaita, G. N.; Hubbard, A. T.; Bent, B. E.; Zaera, F.; Godbey, D.; Samorjai, G. A. *J. Am. Chem. Soc.* **1985**, *107*, 5910−5920.
(8) Batina, N.; Chaffins, S. A.; Gui, J. Y.; Lu, F.; McCargar, J. W.; Rovang, J. W.; Stern, D. A.; Hubbard, A. T. *J. Electroanal. Chem.* **1990**, *284*, 81−96.
(9) Hourani, M.; Wieckowski, A. *Langmuir* **1990**, *6*, 379−385.
(10) Schmiemann, U.; Baltruschat, H. *J. Electroanal. Chem.* **1992**, *340*, 357−363.
(11) Baltruschat, H.; Schmiemann, U. *Ber. Bunsen-Ges. Phys. Chem.* **1993**, *97*, 452−460.
(12) Schmiemann, U.; Müller, U.; Baltruschat, H. *Electrochim. Acta* **1995**, *40*, 99−107.
(13) Müller, U.; Schmiemann, U.; Dülberg, A.; Baltruschat, H. *Surf. Sci.* **1995**, *335*, 333−342.
(14) Baltruschat, H. Differential Electrochemical Mass Spectrometry as a Tool for Interfacial Studies. In *Interfacial Electrochemistry*; Wieckowski, A., Ed.; Marcel Dekker: New York, 1999; pp 577−597.
(15) Berenz, P.; Xiao, X.; Baltruschat, H. *J. Phys. Chem. B* **2002**, *106*, 3673−3680.
(16) Bełtowska-Brzezinska, M.; Łuczak, T.; Mączka, M.; Baltruschat, H.; Müller, U. *J. Electroanal. Chem.* **2002**, *519*, 101−110.
(17) Rodriguez, J. L.; Pastor, E.; Schmidt, V. M. *J. Phys. Chem. B* **1997**, *101*, 4565−4574.
(18) Schmidt, V. M.; Pastor, E. *J. Electroanal. Chem.* **1996**, *401*, 155−161.
(19) Koestner, R. J.; Van Hove, M. A.; Somorjai, G. A. *J. Phys. Chem.* **1983**, *87*, 203-213.
(20) Gabelnick, A. M.; Gland, J. L. *Surf. Sci.* **1999**, *440*, 340−350.
(21) Zaera, F.; Chrysostomou, D. *Surf. Sci.* **2000**, *457*, 71−88.
(22) Zaera, F.; Chrysostomou, D. *Surf. Sci.* **2000**, *457*, 89−108.
(23) Wolter, O.; Heitbaum, J. *Ber. Bunsen-Ges. Phys. Chem.* **1984**, *88*, 2−6.
(24) Wolter, O.; Heitbaum, J. *Ber. Bunsen-Ges. Phys. Chem.* **1984**, *88*, 6−10.
(25) Baltruschat, H.; Bełtowska-Brzezinska, M.; Dülberg, A. *Electrochim. Acta* **1993**, *38*, 281−284.
(26) Biegler, T.; Rand, D. A. J.; Woods, R. *J. Electroanal. Chem.* **1971**, *29*, 269−277.
(27) Wieckowski, A.; Sobkowski, J. *J. Electroanal. Chem.* **1975**, *63*, 365−377.
(28) Herrero, E.; Franaszczuk, K.; Wieckowski, A. J. *Phys. Chem.* **1998**, *98*, 5074−5083.
(29) Sriramulu, S. S.; Jarvi, T. D.; Stuve, E. M. Kinetic Modeling of Electrocatalytic Reactions: Methanol Oxidation on Platinum Electrodes. In *Interfacial Electrochemistry*; Wieckowski, A., Ed.; Marcel Dekker: New York, 1999; pp 793−804.
(30) Iwasita, T.; Pastor, E. A Fourier Transform Infrared Spectroscopy Approach to Double-Layer and Electroanalysis Problems. In *Interfacial Electrochemistry*; Wieckowski, A., Ed.; Marcel Dekker: New York, 1999; pp 353−372.
(31) Windham, R. G.; Bartram, B. E.; Koel, B. E. *J. Phys. Chem.* **1988**, *92*, 2862−2870.
(32) Mohsin, S. B.; Trenary, M.; Robota, H. *J. Phys. Chem.* **1988**, *92*, 5229−5233.
(33) Wong, Y.-T.; Hoffmann, R. *J. Chem. Soc., Faraday Trans.* **1990**, *86*, 4083−4994.
(34) Samorjai, G. A.; VanHove, M. A.; Bent, B. E. *J. Phys. Chem.* **1988**, *92*, 973−978.
(35) Rekoske, J. E.; Cortright, R. D.; Goddard, S. A.; Sharma, S. B.; Dumesic, J. A. *J. Phys. Chem.* **1992**, *96*, 1880−1888.
(36) Backman, A. L.; Masel, R. I. *J. Phys. Chem.* **1990**, *94*, 5300−5308.
(37) Cassuto, A.; Mane, M.; Jupille, J.; Tourillon, G.; Parent, P. *J. Phys. Chem.* **1992**, *96*, 5987−5993.
(38) Müller, U.; Dülberg, A.; Baltruschat, H. *Colloid Surf., A: Phys. Eng. Aspects* **1998**, *134*, 155−164.
(39) Müller, U.; Baltruschat, H. *J. Phys. Chem. B* **2000**, *104*, 5762−5767.
(40) Baltruschat, H.; Staud, N.; Heitbaum, J. *J. Electroanal. Chem.* **1988**, *239*, 361−374.
(41) Patterson, M. L.; Weaver, M. J. *J. Phys. Chem.* **1985**, *89*, 1331−1334.
(42) Patterson, M. L.; Weaver, M. J. *J. Phys. Chem.* **1985**, *89*, 5046−5051.
(43) Feilchenfeld, H.; Weaver, M. J. *J. Phys. Chem.* **1989**, *93*, 4276−4282.
(44) Pastor, E.; Schmidt, V. M. *J. Electroanal. Chem.* **1995**, *383*, 175−180.
(45) Schmidt, V. M.; Pastor, E. *J. Electroanal. Chem.* **1994**, *376*, 65−72.
(46) Zinola, C. F.; Castro Luna, A. M. *J. Electroanal. Chem.* **1998**, *456*, 37−46.
(47) Bełtowska-Brzezinska, M.; Łuczak, T.; Holze, R. *Surf. Sci.* **1998**, *418*, 281−294.
(48) Bełtowska-Brzezinska, M.; Łuczak, T.; Holze, R. J. *Appl. Electrochem.* **1997**, *27*, 999−1011.
(49) Sun, S.-G.; Yang, D.-F.; Tian, Z.-W. *J. Electroanal. Chem.* **1990**, *289*, 177−187.
(50) Pastor, E.; Wasmus, S.; Iwasita, T.; Arévalo, M. C.; González, S.; Arvia, A. J. *J. Electroanal. Chem.* **1993**, *350*, 97−116.
(51) Gootzen, J. F. E.; Wonders, A. H.; Visscher, W.; van Veen, J. A. R. *Langmuir* **1997**, *13*, 1659−1667.
(52) Pastor, E.; González, S.; Arvia, A. J. *J. Electroanal. Chem.* **1995**, *395*, 233−236.
(53) Gootzen, J. F. E.; Wonders, W.; van Veen, J. A. R. *Langmuir* **1996**, *12*, 5076−5082.